



# Corrosion Behaviour of Copper in LiBr Solutions: Effect of Temperature

A. E. El Meleigy<sup>1</sup>, Sh. E. Abd Elhamid<sup>1</sup> and A. A. El Warraky<sup>1\*</sup>

<sup>1</sup>Department of Electrochemistry and Corrosion, National Research Centre, Dokki, Giza, Egypt.

## Authors' contributions

This work was carried out in collaboration between all authors. All authors read and approved the final manuscript.

## Article Information

DOI: 10.9734/BJAST/2015/20045

### Editor(s):

(1) Chang-Yu Sun, China University of Petroleum, China.

### Reviewers:

(1) Anonymous, Universidad Autónoma del Estado de Morelos, Mexico.

(2) Anonymous, V. R. Siddhartha Engineering College, India.

(3) Inemesit A. Akpan, University of Uyo, Uyo, Nigeria.

Complete Peer review History: <http://sciencedomain.org/review-history/11222>

Received 8<sup>th</sup> July 2015

Accepted 12<sup>th</sup> August 2015

Published 1<sup>st</sup> September 2015

Original Research Article

## ABSTRACT

The temperature effect of 25, 50, 70 and 80°C on the dissolution of copper in different concentrations of Lithium Bromide (LiBr) from  $3 \times 10^{-2}$  to 9M was investigated. Three types of corrosion have been detected: General dissolution due to the formation of soluble complex of  $\text{CuBr}_2^-$  between the two anodic peaks (P1 and P2) of the first and second electro-oxidation process; pitting corrosion which occurs after the formation of P2 and the second type of general corrosion form due to autocatalytic dissolution of  $\text{Cu}^+$ . A new type of pitting corrosion known as metastable pitting which depends on temperature and concentration has been detected.

**Keywords:** Copper; LiBr; temperature; pitting corrosion and metastable pitting.

## 1. INTRODUCTION

LiBr heavy brine used as absorbent solution for almost all types of heating and refrigerating absorption systems that use natural gas or steam as, energy sources [1]. Water/LiBr ( $\text{H}_2\text{O}/\text{LiBr}$ ) are

the most commonly used refrigerant/ absorbent couple in absorption systems due to their favourable thermophysical properties [2-4].

Corrosion of copper in concentrated solution of LiBr has been studied in previous work under

\*Corresponding author: E-mail: [el\\_warraky@yahoo.com](mailto:el_warraky@yahoo.com);

different conditions [5-14]. With respect to the advances in refrigeration technology double effect and new triple effect, LiBr absorption machines have been developed. The triple effect absorption chillers are the most logical improvement over the double effect. These chillers exhibit higher elevated operating temperatures than simple effect one and double effect pairs machines.

Several authors have studied the effect of temperature on the galvanic corrosion of different metals and alloys in LiBr concentrated solution such as, high alloyed austenitic stainless steel and its weldment [15] at 150°C, Cu/AISI 304 [16,17] at (25°C-75°C), zinc/copper pair working at (25°C to 85°C) [10], galvanic corrosion of copper at 140°C [9], galvanic corrosion resistance of copper and stainless steel [18], copper alloys [9], alloy 33/ copper and titanium/Cu [18], Cu/xNi [19], galvanic studies of brass and bronzes [20] and analysis of Cu corrosion product at room temperature, 70°C and 110°C [8,21].

Previously [5-7,22], the corrosion behaviour of copper in different concentrations of LiBr was studied using different electrochemical and surface analysis techniques. The results clarify the nature and conditions of film formation, also the composition and difference between the passive film, the partial passive and porous film. The results also discussed the different forms of corrosion recorded at different concentrations up to 9 M at room temperature.

In the present work it is necessary to extend the study to cover the effect of temperature of 25, 50, 70 and 80°C on the dissolution of copper in different concentrations of LiBr ( from  $3 \times 10^{-2}$  up to 9 M). Determination of what condition that is leading to pitting corrosion of copper and also the different forms of corrosion which occur at different temperature. The study comprised electrochemical measurements and surface examination techniques.

## 2. MATERIALS AND METHODS

### 2.1 Selection of Sample Material

Pure copper of 99.99% in the form of rod was used as a test electrode having a working area of  $0.3 \text{ cm}^2$  in contact with the test solution. Before testing, specimens were abraded with emery paper of increasing fineness up to 1000, rinsed in distilled water and degreased with acetone.

The electrochemical cell was made of Pyrex glass with three holes, in which the metal electrode, a platinum auxiliary electrode and saturated calomel electrode (SCE) were fitted. LiBr used is of analytical grade and supplied by Panreac in (Espana). Solutions containing known concentrations of LiBr were obtained by dilutions from stock solutions.

### 2.2 Experimental Design

The electrochemical measurements were carried out with a PS6 Meinsberger Potentiostat/Galvanostat, Germany. Potentiodynamic cyclic polarization curves were recorded in different concentrations of LiBr from  $3 \times 10^{-2}$  to 9 M and at different temperatures of 25, 50, 70 and 80°C. Before polarization measurements, the sample was kept at -800 mV versus saturated calomel electrode (SCE) for 20 min. in the test solution to reduce the pre-immersion oxides on the sample surface. The potentiodynamic cyclic polarization test was carried out by scanning the potential of the electrode from -800 mV towards noble values up to 2000 mV using a scanning rate of 1 mV/sec and reversed again to the backward direction with the same scanning rate.

Some of the samples were taken after polarization treatment to a definite potential for surface analysis, where the samples were cleaned in bidistilled water for 30 min. using ultrasonic vibration, dried between fibreless tissues, coated with gold and immediately introduced into the vacuum chamber of a scanning electron microscope (SEM) Model Philips XL 30 (XL 30, Philips, Netherlands) Made in 5600MD Eindhoven-Holanda attached with energy dispersive x-ray (EDX) Unit, with accelerating voltage 30 K.V., magnification 10x up to 400.000x and resolution for W. (3.5 nm). The changes of films were complemented by optical microscope (O.M) (Olympus Bx-51. Japan).

## 3. RESULTS AND DISCUSSION

### 3.1 Diluted Solutions of LiBr

The curves of Fig. 1 represent the cyclic polarization of copper in  $3 \times 10^{-2}$  M LiBr at temperatures varying between 25°C and 80°C. Fig. 1(a) shows that at 25°C,  $E_{\text{Corr}}$  recorded at less negative value of -140mV as shown in Table 1. At such concentration the anodic reaction is essentially limited by the applied potential where

the bromide ions have little significant effect as mentioned previously [5]. While the dissolution of copper can take place through the formation of  $\text{CuBr}_2^-$  soluble copper complex [5,6,8,23,24]. The curve shows also that the dissolution current increases linearly with potential, revealing that the dissolution reaction is charge transfer controlled. The appearance of the plateau of current with increasing potential represent that the dissolution reaction is controlled by mass transport of  $\text{CuBr}_2^-$  through  $\text{CuBr}$  film [23,25-27].

By increasing the temperature from 25°C to 80°C, Fig. 1(b), different features can be distinguished. First, the cathodic branch recorded a plateau in the current density which is increased with increasing temperature. Therefore, the cathodic reaction seems to be controlled by diffusion [24]. Second, the corrosion potential is shifted to more negative value as shown in Table 1. Third, the appearance of the two anodic peaks (P1 and P2) of the first and the second electro-oxidation process of Cu (I) and Cu (II) as recorded previously [22]. Fig. 1(b), at 80°C shows that the potential of P1 ( $E_{P1}$ ) was recorded at 70 mV while the potential of second peak P2 ( $E_{P2}$ ) at 950 mV as shown in Table 1. After ( $E_{P2}$ ), the current density is decreased from 10 to 4 mA/cm<sup>2</sup> suggesting the formation of a protective film of copper oxide. This occurs as a result of oxidation of  $\text{Cu}_2\text{O}$  to  $\text{CuO}$  and/or  $\text{Cu}(\text{OH})_2$  [5]. The second peak (P2) was followed by fluctuations, which

extended to the end of the experiment. These fluctuations are similar to that recorded previously by many researchers [20,28-34]. They concluded that before pitting of metals and alloys some small current fluctuation occurs, which are defined as metastable pitting. This type of pitting is recorded previously in case of stainless steels and aluminum alloys [28,26-39]. It is well known that, metastable pitting is one form of pitting corrosion where pits are initiated and grow for limited small time before the surface become re-passivated. Accordingly, the fluctuation recorded in Fig. 1(b) is called metastable pitting, as will be confirmed later. Here the bromide concentration is not sufficient to attack the formed film through pitting corrosion.

Fig. 2(a) shows the effect of  $4 \times 10^{-2}$  M of LiBr concentration at 25°C on the dissolution of Cu. The figure represents that  $E_{\text{Corr.}}$  was shifted to more negative value while  $i_{\text{Corr.}}$  was increased to 0.5 mA/cm<sup>2</sup>. On the other hand both P1 and P2 were formed at  $E_{P1}=100$  mV and  $E_{P2} = 1350$  mV due to the formation of the higher oxidation state of  $\text{CuO}$  and  $\text{Cu}(\text{OH})_2$  [5]. These results reveal that before  $E_{P2}$  general dissolution takes place whereas after  $E_{P2}$  a sharp decrease in current was recorded. The decrease in current detected can reasonably be related to the formation of the higher oxidation state which is more passive and protective. Increasing the temperature from 25°C to 50°C, 80°C,  $E_{\text{Corr.}}$  was shifted to more negative

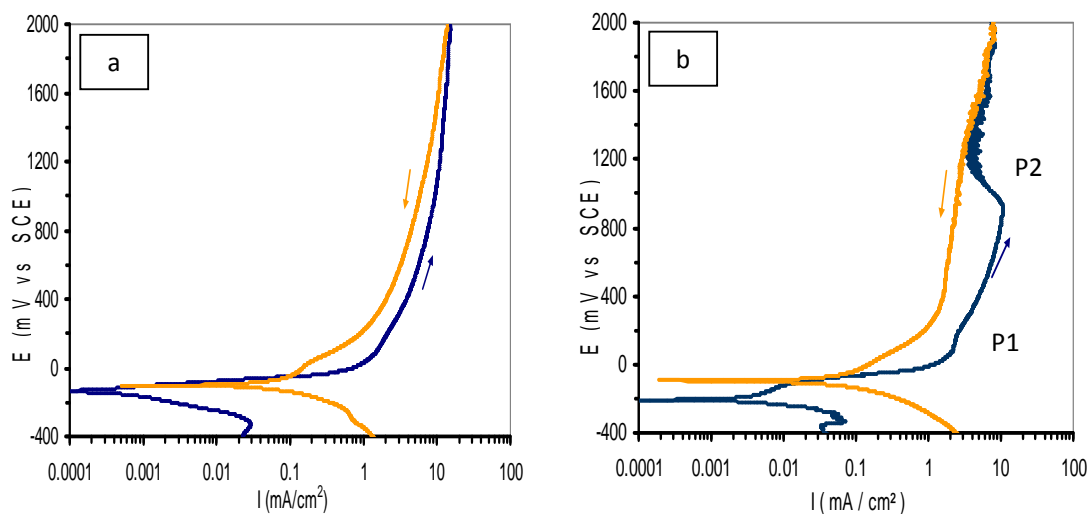
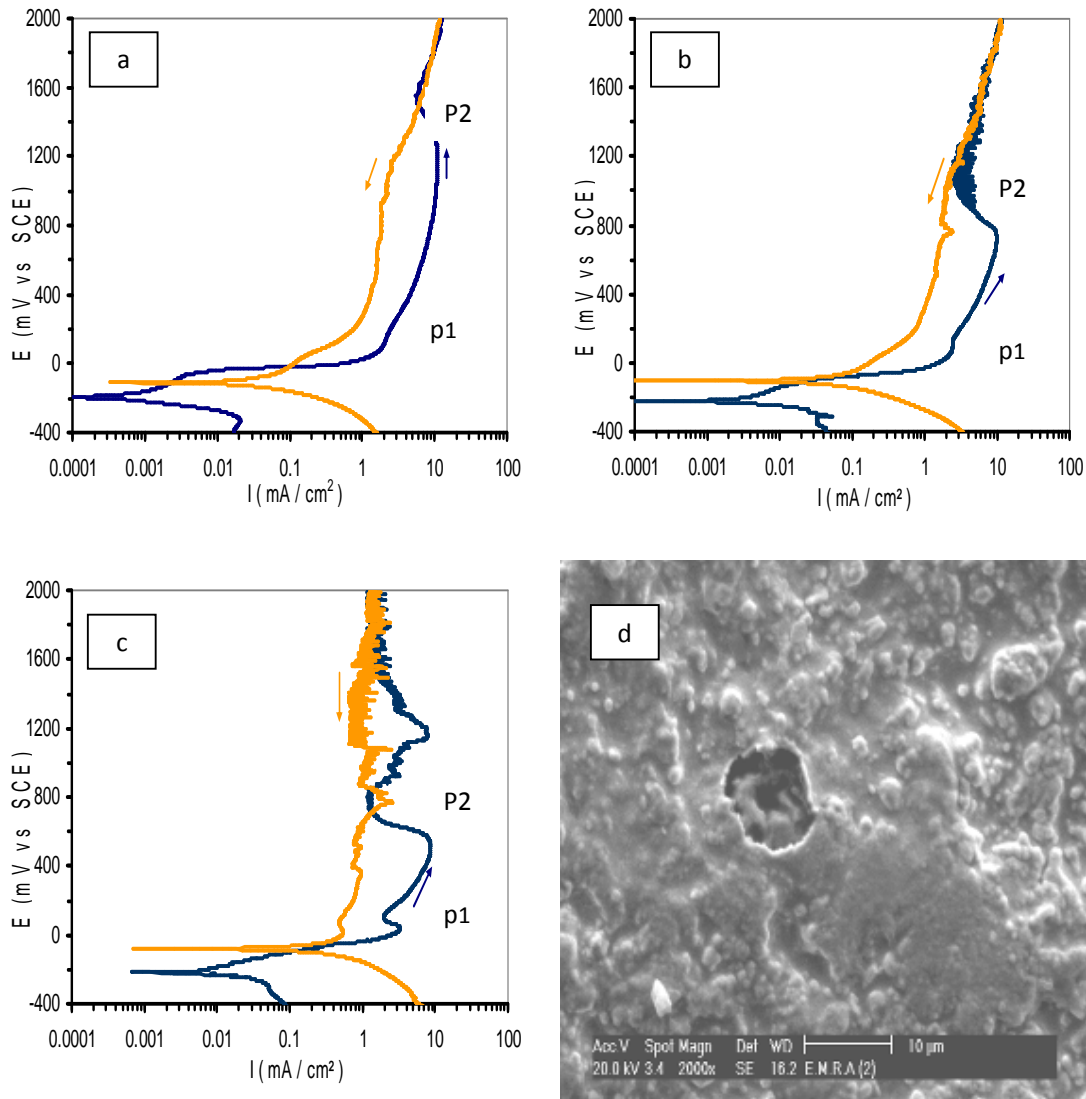


Fig. 1. Cu in  $3 \times 10^{-2}$  M LiBr at different temp.; a (25°C), b (80°C)



**Fig. 2. Cu in  $4 \times 10^{-2}$  M LiBr at different temp.:** a (25°C), b (50°C), c (80 °C), d (SEM for Cu at 80°C)

potentials and a maximum shift was achieved at 80°C Fig. 2(c). This is accompanied by an increase in the corrosion current from 0.5 to 0.8 and 1 mA/cm<sup>2</sup> corresponding to 25°, 50° and 80°C, respectively as shown in Table 1. In contrast,  $E_{P1}$  and  $E_{P2}$  were shifted to less positive potential by increasing temperature and consequently, metastable pitting region is increased.

Further insight into the different forms of corrosion could be gained using SEM technique. Examination of the surface of Cu specimen after polarization in  $4 \times 10^{-2}$  M LiBr at 80°C (within the metastable pitting region) is shown in Fig. 2(d).

The picture showed that one of initiated and repassivated pit was recorded without any porous structure. As mentioned previously in experimental, the ultrasonic vibration method is used for cleaning the sample surface. This means that not all the corrosion product are removed and the detection of one or more initiated and repassivated pit give an indication of the metastable pitting. On the other hand, the porosity of the film formed are taken from the micrographs of SEM relative to each other and not deduced. The above result means that along the metastable pitting region, the film cannot reach to a stable passivation where initiation and repassivation are simultaneously occurring.

These results are in agreement with the previous published data [39], in case of dilute Al-Cu solid solution alloys, which concluded that the metastable pit transient during potentiostatic polarization near to, but below the pitting potential showed that the slow repassivation depresses the metastable pit initiation and growth rates which decrease the probability of formation of stable pits.

Considering the solution of LiBr concentration  $8 \times 10^{-2}$  M at 25°C, the curve of Fig. 3(a) and Table 1 represent that there are other shift in  $E_{\text{Corr.}}$  to more negative potential (-194mV) while  $i_{\text{Corr.}}$  was increased to become 1.5mA/cm<sup>2</sup>. While  $E_{\text{P1}}$  and  $E_{\text{P2}}$  were recorded at 60 and 750mV respectively and the hysteresis loop area was produced. Rising the temperature of  $8 \times 10^{-2}$  M LiBr solution to 50°C, as shown in Fig. 3(b) and Table 1,  $E_{\text{Corr.}}$  was shifted to 200mV and  $i_{\text{Corr.}}$  increased to 1.7 mA/cm<sup>2</sup> while  $E_{\text{P1}}$  and  $E_{\text{P2}}$  were shifted to less positive potentials. The important feature recorded at this temperature (50°C) is the breakdown after the metastable pitting region which yields a small hysteresis loop area where  $E_{\text{pit.}}$  was recorded at 1300 mV and the repassivation potential ( $E_{\text{rp.}}$ ) at 900 mV. The increase in the current density which occurs due to the breakdown is associated with a continuous oscillation after  $E_{\text{pit.}}$ . The SEM the micrograph of Fig. 3(e) at 50°C shows that not all the surface reach to a passivation state where some pits can propagate at different weak points as shown in the dark black area at the upper right region on the picture. Also some regions on the surface are still in the metastable pitting state as clear on the left of the picture in the form of four metastable pits. It is well known the passivation, passive current and partial passive current, protective film, non protective film and the different type of corrosion recorded were gained mainly from the polarization measurement and surface examination using EDX and O.M. The SEM was used to confirm the results of the other techniques. Another rising in the temperature to 70°C and 80°C, Fig. 3(c,d) and Table 1 shows the same features which were recorded at diluted concentrations with some changes in the values recorded at all parameters. From the above, we can conclude that as increasing the temperatures  $E_{\text{Corr.}}$  was shifted to more negative potential while  $i_{\text{Corr.}}$  was increased and both of P1 and P2 were formed with higher rate at less positive potential. After  $E_{\text{P1}}$  the dissolution of Cu occurs by general form through the porous CuBr and/or Cu<sub>2</sub>O film suggesting that, the first electro-oxidation involved a certain mass transport of reactive

through the pores in the base film [40,41]. This is expected because the temperature enhances the mass transport by diffusion [2,24,42]. This behaviour is extended until P2 recorded where a protective film of Cu (II) oxide is formed as reported previously [5] and confirmed later in Table 2.

After the formation of P2, Fig. 3, the dissolution of Cu occurs by metastable pitting which in some cases a breakdown in this film occurs and pitting corrosion was produced. This occurs at definite sites on the surface depending on the defective points and the effect of temperature. This is in agreement with a recent published data [28,43] which shows that the process of pitting corrosion in similar condition may be divided into a sequence of steps: First, micro-pits initiate due to local breakdown of the passive film. Second, most of the micro-pits would repassivate after short growth, but some may develop into stable pitting corrosion. At higher temperature, 70°C and 80°C after P2, Fig. 3(c,d) shows that the dissolution was occurred by the metastable pitting only without any breakdown. This fact occurs because the passive film became more protective with increasing the temperature. The passive film formed at lower temperature after P2 is CuO and Cu(OH)<sub>2</sub> [5] which is more defective and less resistance to film breakdown than those formed at higher temperature which is mainly CuO. This behaviour is in agreement with that reported previously [8,41,44] which show that, by temperature Cu(OH)<sub>2</sub> is not stable thermodynamically which tends to transformed to CuO by dehydration and forming a passive film of more compact and less porous structure. On the other hand, it is well known that as the solution temperature increases the dissolved oxygen in solution decreases [8,45]. This fact decreases the cathodic reaction rate, which occurs by the reduction of oxygen on the cathodic sites as:-



On the other hand, as discussed previously [8,15], the temperature enhances the diffusion and transport of the product to or from the metallic surface. The above three reasons are responsible on the elongation of the metastable pitting area at 70°C and 80°C. This is extended till the end of the experiment without any breakdown where equilibrium in the initiation of pits and repassivation was attained. Another confirmation was gained from measuring the current fluctuation as shown in Fig. 4.

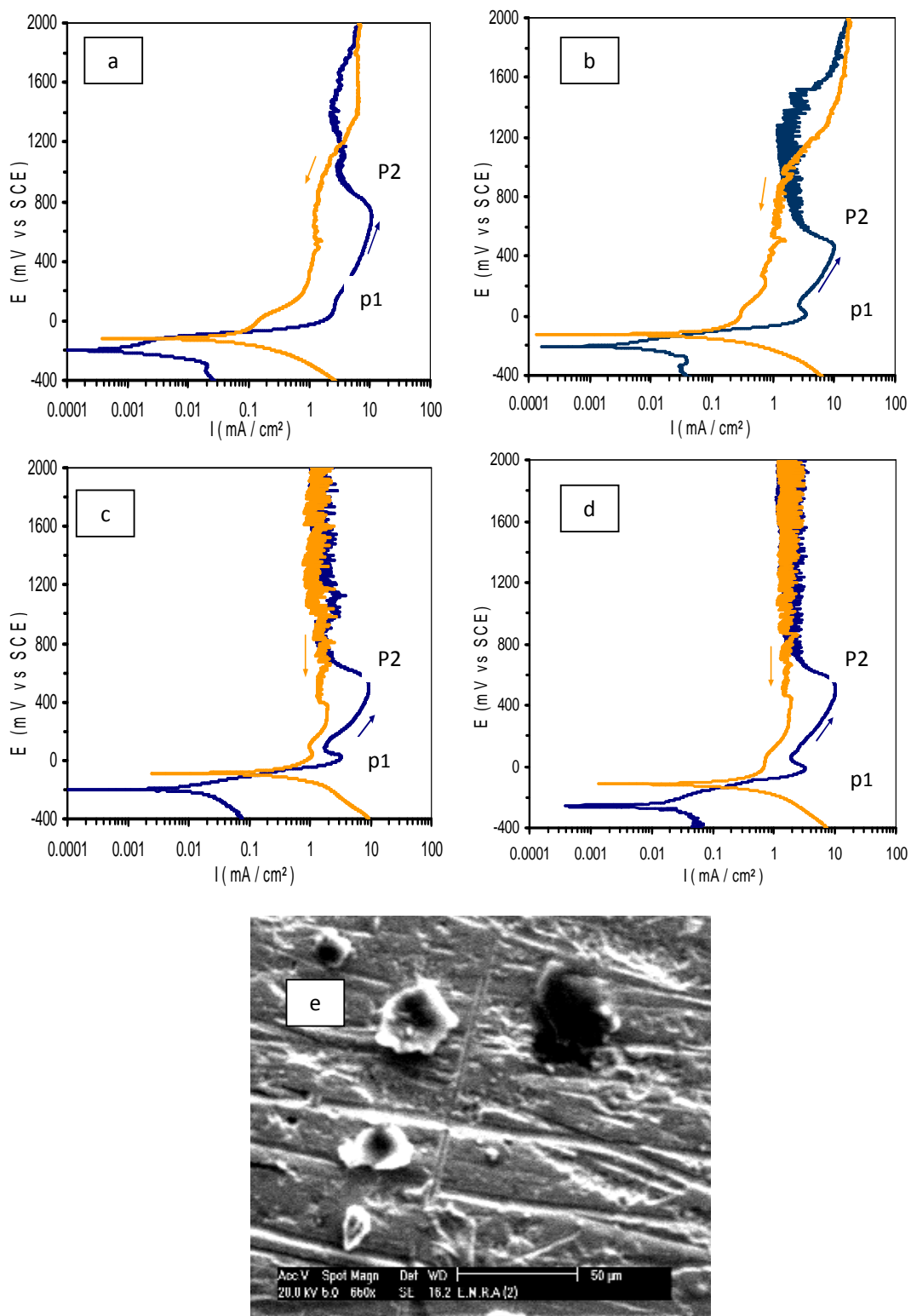


**Fig. 3.** Cu in  $8 \times 10^{-2}$  M LiBr at different temp.; a (25°C), b (50°C), c (70 °C), d (80 °C), e (SEM for Cu at 50 °C)

Previous studies [28,38] analyzed the current fluctuations of stainless steel and the probability of transition from metastable pitting to stable propagation. Frankel et al. [32] found that, the metastable pitting is transformed to a stable pit when the dissolution current and pit radial reaches  $4 \text{ mA/cm}^2$ . Others [46-49] suggested a stable pitting occur after  $3 \text{ mA/cm}^2$ . Fig. 4(a) shows the current fluctuations during the first 100 mV of the metastable pitting region of Fig. 3(c) which is recorded at  $70^\circ\text{C}$ . Tang et al. [28] used the peak current instead of the electric current because the initial pit repassivates very quickly.

Therefore, the peak current of fluctuation of Fig. 4(a) which is  $0.425 \text{ mA/cm}^2$  is considered as a metastable pitting process. On the other hand, Fig. 4(b) recorded during the first 100mV of the metastable pitting region of Fig. 3(b) which was recorded at  $50^\circ\text{C}$  before the  $E_{\text{pit}}$ . The increase in the peak current of fluctuation to  $1.13 \text{ mA/cm}^2$  as calculated from Fig. 4(b) confirms that the initiated pits are developed which acts on the continuous dissolution and the metastable pitting would transformed to a stable pit as shown in Fig. 3(b).

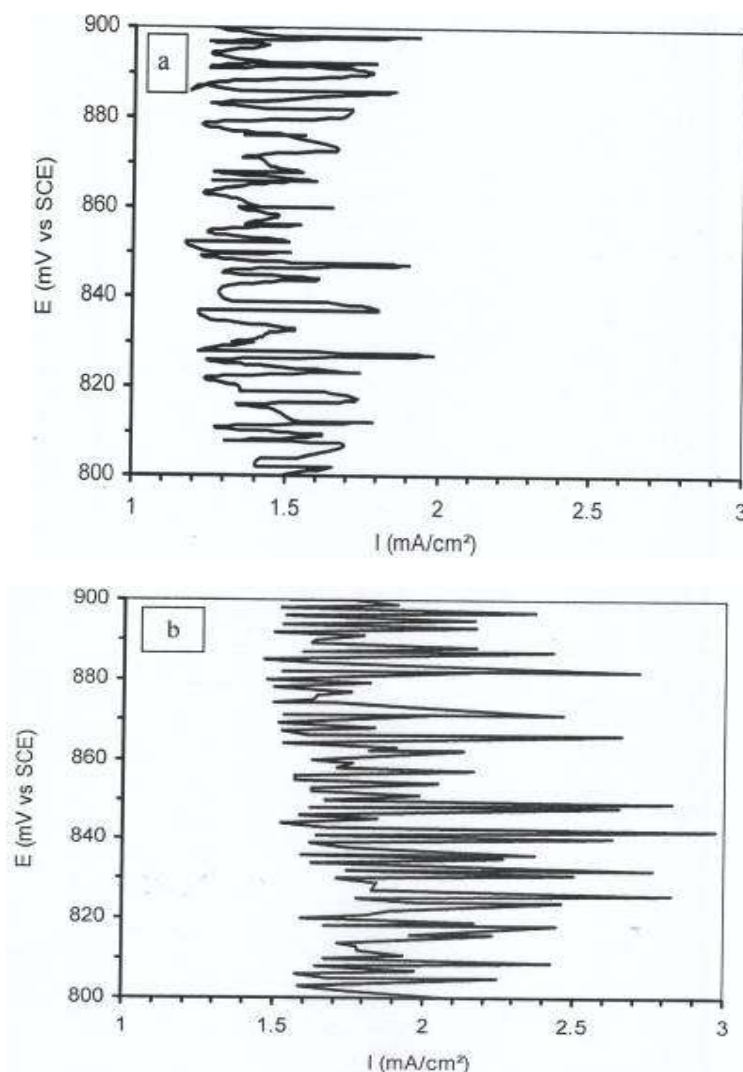


**Fig. 4. Polarization curve of Cu in  $8 \times 10^{-2} \text{ M LiBr}$  during the first 100mV of the metastable pitting region (a) In Fig. 3(c); (b) In Fig. 3(b)**

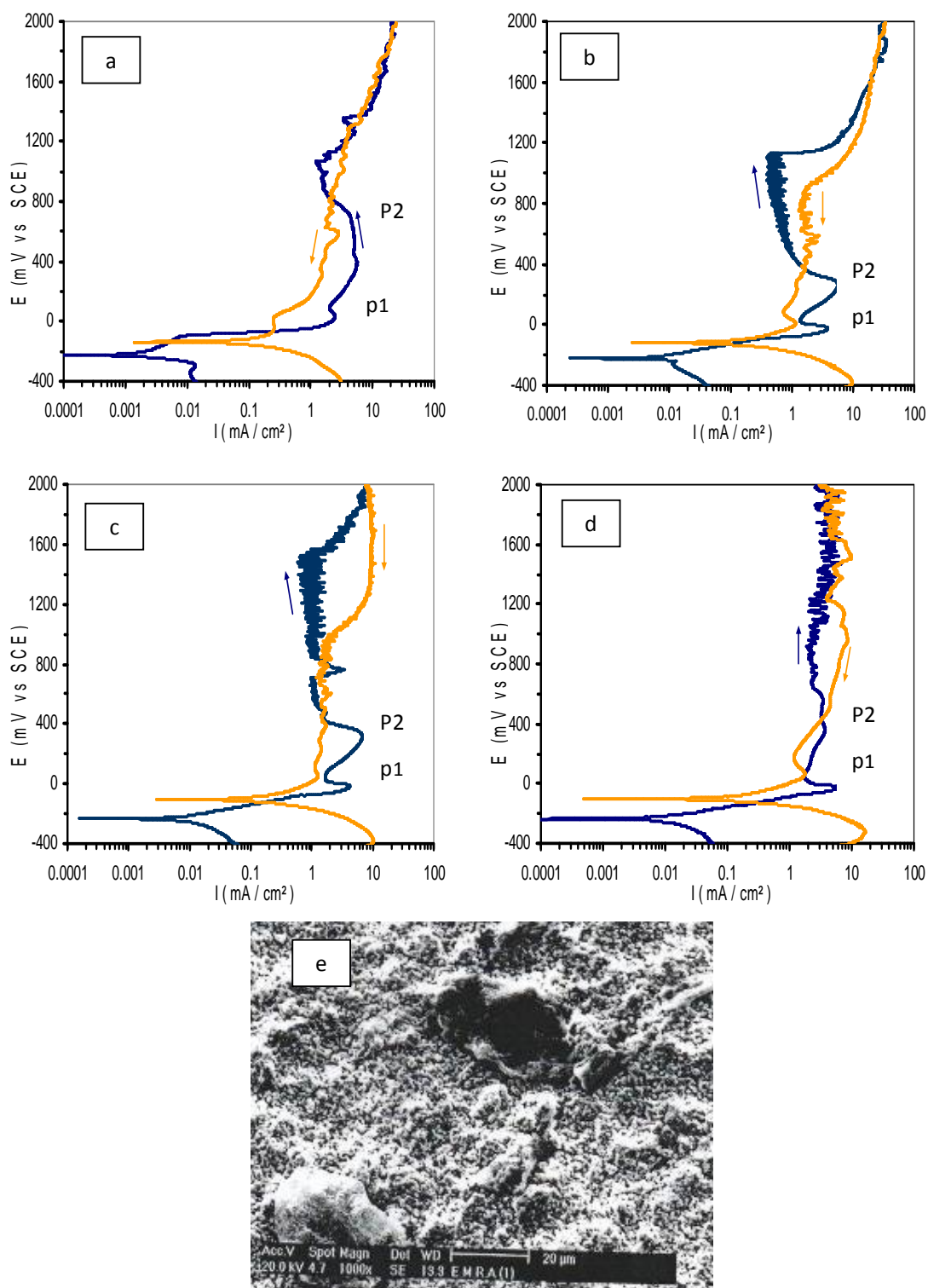


Fig. 5. Cu in  $10^{-1}$  M LiBr at different temp.; A (25°C), b (50°C), c (70 °C), d (80 °C), e (SEM for Cu at 50 °C (E = 1400mV))

The curves of Fig. 5(a-d) exhibit the cyclic polarization behaviour of Cu in  $10^{-1}$ M LiBr solution at different temperatures. The curves at each temperature show another two features than those recorded in corresponding temperature at less concentrated solutions. The first feature is about  $E_{Corr}$ . this does not show any shift by increasing the temperature from 25°C to 80°C, Fig. 5 and Table 1. The second feature is the small difference in potential recorded between  $E_{P2}$  and  $E_{P1}$ . The decrease in this region

by increasing the temperature means that general dissolution represents a small part with respect to the pitting corrosion where, a large hysteresis loop area was recorded as shown in Fig. 5 (b,c) and Table 1. Examination of the treated sample at 1400mV (after breakdown potential) of experiment of Fig. 5(b) at 50°C using SEM, as represented in Fig. 5(e), the surface was covered with a continuous adherent film where some stable pits were recorded confirming that the dissolution occur mainly by stable pitting.

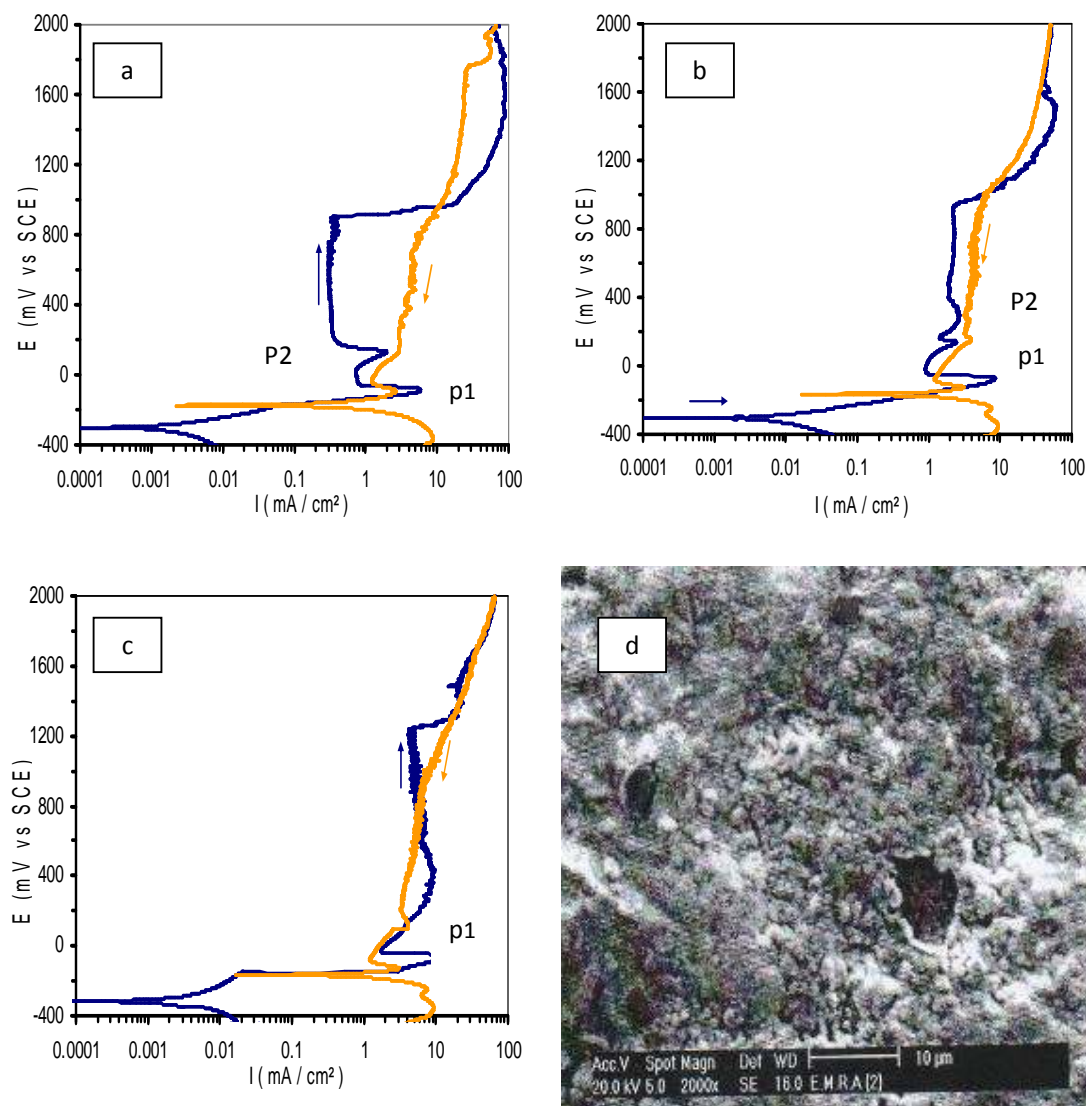


Fig. 6. Cu in  $5 \times 10^{-1}$ M LiBr at different temp.; a (25°C), b (50°C), c (80 °C), d (SEM for Cu at 25°C (E = 1200mV))

From Fig. 6 and Table 1 at  $5 \times 10^{-1} \text{ M LiBr}$ , reveal that with increasing the temperature  $E_{\text{Corr}}$  is still at the same value while  $i_{\text{Corr}}$  was increase.  $E_{\text{P1}}$  was recorded nearly at the same negative value as increasing the temperature. While  $P_2$  was recorded at  $25^\circ\text{C}$  and  $50^\circ\text{C}$  only (Fig. 6(a, b)) at the same value (180 mV) which disappeared at  $80^\circ\text{C}$ , Fig. 6(c). The difference between  $E_{\text{P2}} - E_{\text{P1}}$  is very small at  $25^\circ\text{C}$  and  $50^\circ\text{C}$  which represents that there is no chance for the general dissolution between them. This is followed by a sharp passive region, which shows a something metastable pitting and the breakdown in the formed film were recorded where,  $E_{\text{pit.}} = 920$  and  $950$  mV at  $25^\circ$  and  $50^\circ\text{C}$  respectively, Fig. 6 (a, b). These values are less positive in comparison with those recorded previously at the corresponding temperature of less concentrated solutions. On the other hand, the hysteresis loop area was decreased while the value of the passive current density was increased as increasing the temperature, Fig. 6(c).

Fig. 7 shows the forward anodic polarization of the cyclic of Fig. 6(a-c). The curves in Fig. 7 show that  $P_1$  was formed at all temperatures while a larger peak of  $P_2$  was recorded at  $25^\circ\text{C}$ . This is followed by a higher decrease in the current after the formation of  $P_2$  ( $0.3 \text{ mA/cm}^2$ ). This means that the passive film is mainly  $\text{CuO}$  where the electrode surface is covered with black  $\text{CuO}$  film and a small ratio of blue  $\text{Cu(OH)}_2$ , as

represented in Table 2. At  $50^\circ\text{C}$  in Fig. 6(b),  $P_2$  became very small which is followed by slow increase in the current and the partially passive current density was recorded at ( $2.3 \text{ mA/cm}^2$ ). As shown in Table 2, the species at  $50^\circ\text{C}$  is mainly  $\text{CuO}$  with small ratio of  $\text{Cu}_2\text{O}$ . At higher temperature of  $80^\circ\text{C}$  as shown in Fig. 6(c),  $P_2$  was disappeared while a partial passive current was recorded at higher value ( $6 \text{ mA/cm}^2$ ). Table 2 confirmed the above results where, the species recorded at  $80^\circ\text{C}$  are mainly  $\text{Cu}_2\text{O}$  with small ratio of  $\text{CuO}$  which is partially protective.

To discuss the above results at  $10^{-1}$  and  $5 \times 10^{-1} \text{ M LiBr}$  it is necessary to mention two reasons which are discussed previously, the first reason represent that increasing the temperature transferred  $\text{Cu(OH)}_2$  to  $\text{CuO}$  by dehydration which increased the passivity and the surface become more protective. This is behind the formation of the passive current density at low value ( $0.3 \text{ mA/cm}^2$ ) which is recorded previously at  $10^{-1} \text{ M LiBr}$  at  $50^\circ\text{C}$  and  $70^\circ\text{C}$  of Fig. 5(b,c). While the second reason represents that, there is a decrease in the dissolved oxygen by temperature and in contrary; the temperature enhances the diffusion and the mass transport of the product to or from the metallic surface [8]. Fig. 7 shows that the passive current density recorded at  $25^\circ\text{C}$  was changed to partially passive as increasing the temperature where  $P_2$  was disappeared at  $80^\circ\text{C}$  as shown in Fig. 7(c).

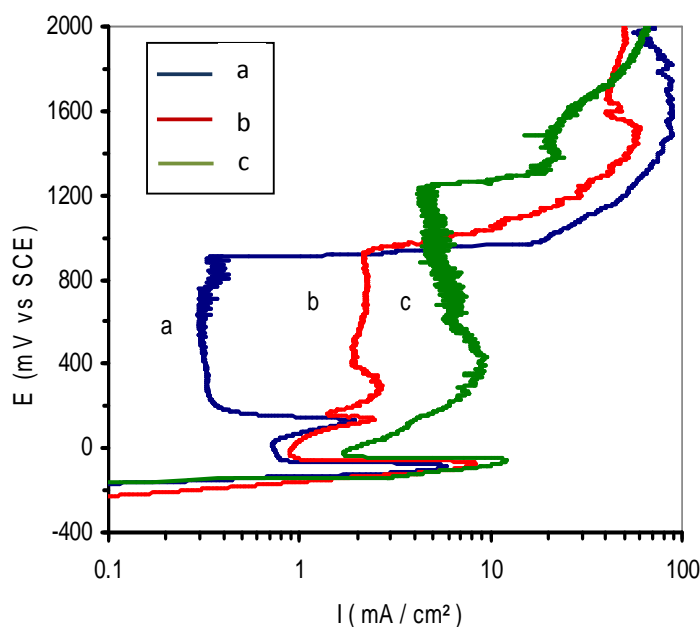


Fig. 7. Cu in  $5 \times 10^{-1} \text{ M LiBr}$  at different temp.; A ( $25^\circ\text{C}$ ), b ( $50^\circ\text{C}$ ), c ( $80^\circ\text{C}$ )

This occur as previously recorded in  $5 \times 10^{-1}$  M LiBr of Fig. 6(b,c) at 50°C and 80°C, the deficiency in oxygen is not effective enough in comparison with the increase in the diffusion and mass transport which occur with higher rate as increasing the temperature. These tends to increase the anodic reaction specially through the CuBr or Cu<sub>2</sub>O which cannot oxidized to CuO and/or Cu(OH)<sub>2</sub> [50]. This confirms that at  $5 \times 10^{-1}$  M LiBr, of 50°C the dissolution of Cu is mainly pitting which is accompanied by some ratio of general corrosion. This occurs as a result of the formation of CuO with some amount of Cu<sub>2</sub>O as represented in Table 2 which confirmed by SEM of Fig. 6(d). While at 80°C the dissolution is

mainly general where, the breakdown is occur as a result of the autocatalytic reaction as represented later in concentrated solutions of LiBr.

### 3.2 Concentrated Solutions of LiBr

The anodic polarization curves of copper in 1M LiBr at different temperatures are displayed in Fig. 8. It should be noted that at 25°C, Fig. 8(a), each of (P2), the passive region of low current density ( $0.3 \text{ mA/cm}^2$ ), the metastable pitting and pitting corrosion were not recorded while a partial passive current was recorded with higher value.

**Table 1. Corrosion potentials ( $E_{corr}$ ), corrosion current densities ( $i_{corr}$ ), the potentials of the two peaks ( $E_{P1}$  and  $E_{P2}$ ) and the potential difference between the two peaks ( $E_{P2} - E_{P1}$ ) of potentiodynamic polarization of Cu in different concentrations of LiBr and at different temperatures**

Conc. (M)	Temp. (°C)	$E_{corr}$ (mV)	$i_{corr}$ (mA/cm <sup>2</sup> )	$E_{P1}$ (mV)	$E_{P2}$ (mV)	$E_{P2} - E_{P1}$ (mV)
$3 \times 10^{-2}$	25°C	-140	0.35	----	----	----
	80°C	-210	0.7	70	950	880
$4 \times 10^{-2}$	25°C	-190	0.5	100	1350	1250
	50°C	-220	0.8	70	780	710
$8 \times 10^{-2}$	80°C	-215	1	30	520	490
	25°C	-194	1.5	60	750	690
	50°C	-200	1.7	10	480	470
	70°C	-200	2	20	520	500
$1 \times 10^{-1}$	80°C	-265	2	-20	500	520
	25°C	-225	1.4	40	720	680
	50°C	-225	2	-20	280	300
	70°C	-225	2	-20	280	300
$5 \times 10^{-1}$	80°C	-225	2.5	-20	380	400
	25°C	-302	3	-80	180	260
	50°C	-302	3.5	-70	180	250
	80°C	-302	4	-70	----	----

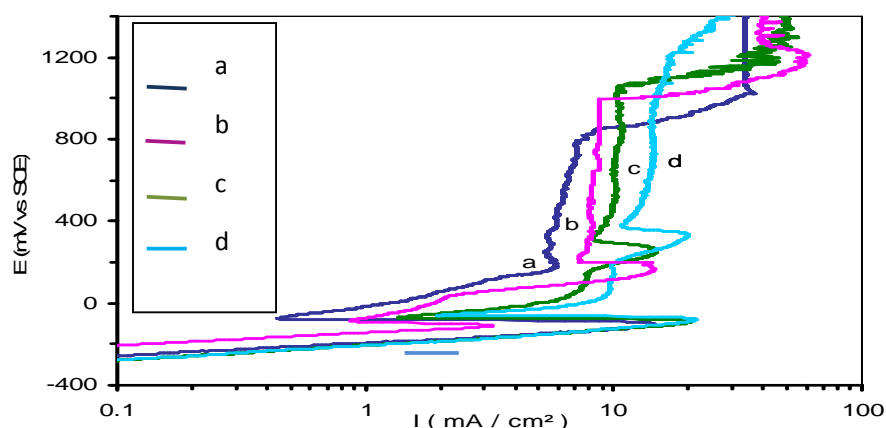


**Fig. 8. Cu in 1M LiBr at different temp.; A (25°C), b (50°C), c (70 °C), d (80 °C)**

**Table 2. Surface examination of Cu after potentiodynamic polarization measurement in different concentrations of LiBr solutions and at different temperatures**

Conc. Of LiBr (M)	SEM at 25°C	EDX at 25°C			O.M at t °C			I mA/cm <sup>2</sup> at t °C			Chemical species on Cu Surface, t °C		
		Cu%	O%	Br%	25	50	80	25	50	80	25	50	80
5x10 <sup>-1</sup> M at 200 mV (at the passive region)	Non porous film	68.8	30.42	traces	b.>> bl.	b. and red	red>> b.	0.36	2	5.95	CuO>> Cu(OH)2	CuO> Cu2O	CuO2>CuO
1M at 600 mV(at the partial passive region)	Porous film	67.7	31.6	--	red color with a traces of y. and bl.	red > w.	red < w.	6.52	8.2	13.87	Cu <sub>2</sub> O >> Cu(OH) and Cu(OH)2	Cu2O> CuBr	CuO2 < CuBr
1 M at 1000 mV	Non-homo. corr. product	54.2	13.55	32.23	b. and red at some area	w., b. and traces redd.	w., b.	31.2	14.8	14.31	CuBr2 (due to the del. effect of Br on cu2O)	Cu Br CuBr2 and traces Cu2O	CuBr, CuBr2
2 M at 100 mV	Quit hom. and less porous than 1M	56.7	23.78	19.49	redd. > w. >>> b.	w., b.	w., b.	8.5	17.6	41.35	Cu2O> CuBr and traces of CuO	CuBr, CuBr2	CuBr, CuBr2
2 M at 400 mV	Non-homo. and more porous	43.7	22.16	34.14	w.>>>> b. and traces of other Cu salts	w., b.	w., b.	13.9	24.9	38.33	CuBr and traces CuO and / or Cu (OH)2	CuBr, CuBr2	CuBr, CuBr2
4 M at 400 mV	dis. loosely adh. corr. product	61.6	1.44	36.92	mainly w. >>> y. and bl.	w., b.	w., b.	38	80	100	CuBr and traces CuOH and Cu(OH)2	CuBr, CuBr2	CuBr, CuBr2
6 M at 400 mV	Non-homo. And less adh.	65	1	34	W. >>> b.	W. and b.	W. and b.	75	100	140	CuBr, CuBr2	CuBr, CuBr2	CuBr, CuBr2
9 M at 400 mV	Non-homo. And less adh.	62	---	38	W. >>> b.	W. and b.	W. and b.	110	150	190	CuBr, CuBr2	CuBr, CuBr2	CuBr, CuBr2

Abbreviations: t = temperature hom. = homogenous corr. = corrosion del. = deleterious dis. =discontinuous adh. = adherent redd. = reddish b = black y = yellow bl = blue w = white

This occurs as a result of competition between the Cu<sub>2</sub>O film formed and the dissolution of the metal through the formation of CuBr<sub>2</sub><sup>-</sup> soluble complex. After 850 mV, the breakdown in potential is due to the higher general dissolution as a result of the formation of Cu<sup>2+</sup> soluble species during the autocatalytic reaction [5,6,41] as



Increasing the temperature to 80°C affects the dissolution where as shown in Fig. 8 and Table 3, there is no changed in E<sub>corr.</sub> and E<sub>P1</sub> while i<sub>corr.</sub> was increased with temperature. On the other hand, both the current density (i<sub>P1</sub>) recorded at E<sub>P1</sub> and during the partial passive region was increased. This confirms the above result, which shows that as increasing the temperature the length of the partial current region and the current densities values were increased. Table 2 represented that at 80°C, the species formed on the surface are Cu<sub>2</sub>O and CuBr at 600 mV while at 1000 mV its CuBr and CuBr<sub>2</sub><sup>-</sup> where these species are formed as a result of deleterious effect of bromide. These confirmed the previous study (22) of autocatalytic dissolution as in equation (2) and or the deleterious effect of bromide on Cu<sub>2</sub>O as



To confirm the above result also the concentration of LiBr is increased to 2M at different temperature of 25, 50, 80°C as shown in Fig. 9. At these conditions, the electrode potential was scanned from -600 to 800 mV only to maintain the decrease in the sample area. The curves of Fig. 9 and Table 3 show that by increasing the temperature, all the parameters of Table 3 were shifted to higher values. As shown in Fig 9 (a) and Table 2 at concentration of 2M at 25° C, the film formed is non-homogeneous with a more porous structure than those recorded at corresponding diluted one. In addition, the EDX analysis recorded at 25°C, as in Table 2, indicate that the presence of Cu, O and Br with atomic concentration percentage of 43.7, 22.16 and 34.14 respectively on the surface at the partial passive region (400 mV).

As increasing the concentration of LiBr to 4, 6 and 9 M, potentiodynamic polarization measurements show nearly the same trend as those recorded at 2 M LiBr. Table 3 represented that as increasing both of the concentration and temperature, E<sub>corr.</sub> was shifted to more negative direction and i<sub>corr.</sub> was increased while E<sub>P1</sub> was shifted to less negative direction. On the other hand, Table 2 shows that first, the film formed is non-homogenous and became non adherent where, some of the corrosion products are laid out the surface to the bottom of the cell. Second, the EDX analysis and O.M examination proved that the species present on the surface of Cu after polarization to 400 mV are CuBr and CuBr<sub>2</sub>.

**Table 3. corrosion potentials (E<sub>corr.</sub>), corrosion current densities (i<sub>corr.</sub>), Potential of the first peak (E<sub>P1</sub>) and current of the first peak (i<sub>P1</sub>) for potentiodynamic polarization of Cu in different concentrations of LiBr and at different temperatures**

Conc. (M)	Temp. (°C)	E <sub>corr.</sub> (mV)	i <sub>corr.</sub> (mA/cm <sup>2</sup> )	E <sub>P1</sub> (mV)	i <sub>P1</sub> (mA/cm <sup>2</sup> )
1	25°C	-350	6	-100	15
	50°C	-330	7	-100	17
	70°C	-360	9	-100	20
	80°C	-350	12	-100	20
2	25°C	-370	7	-120	24
	50°C	-375	12	-100	34
	80°C	-400	20	-100	60
4	25°C	-470	20	-100	-----
	50°C	-480	35	-80	-----
	80°C	-500	55	-90	-----
	25°C	-480	30	-80	-----
6	50°C	-500	42	-90	-----
	80°C	-530	68	-80	-----
	25°C	-500	60	50	-----
9	50°C	-550	80	40	-----
	80°C	-580	110	40	-----

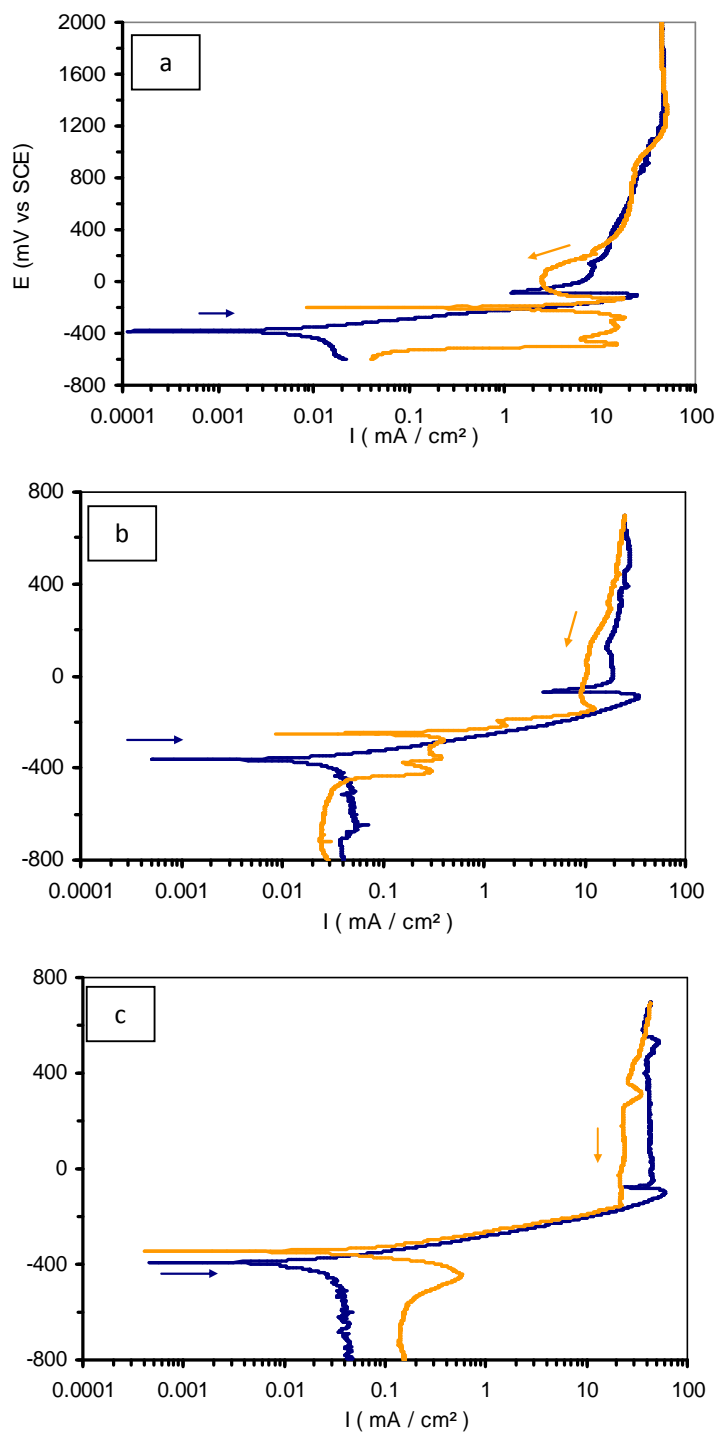


**Fig. 9. Cu in 2M LiBr at different temp.; a (25°C), b (50°C), c (80 °C)**

As it is widely known, as the temperature increases both the charge and mass transfer occur with higher rate through the weaker layer of CuBr, which enhances both cathodic and anodic reactions. In contradiction, the decrease in the dissolved oxygen solubility, which retards the cathodic reaction, is very small in comparison with the enhancement of both cathodic and

anodic reactions at these concentrated solutions of LiBr. These factors are responsible on the general dissolution of Cu at concentrated solutions up to 9 M as a result of formation of CuBr and CuBr<sub>2</sub> as in Table 2 through the reaction (2, 3, and 5). The concentration of 9 M LiBr is equivalent to the ≈ 850 g/l which is the commonly adopted as absorbent solution for refrigerating absorption systems.

## 4. CONCLUSION

### 4.1 Diluted Solutions of LiBr

- i. The polarization curves which are recorded in  $3 \times 10^{-2}$  M LiBr at 25°C and 50°C indicates that at 50°C, the corrosion potential was shifted to more negative value and the second electro-oxidation process was appeared at more positive potential. This is followed by the metastable pitting corrosion which extended to the end of the experiment.
- ii. By increasing the concentration of LiBr to  $4 \times 10^{-2}$  M and up to 80°C, the dissolution of Cu occurs by general corrosion in the region between P1 and P2 and after P2 metastable pitting was produced.
- iii. At of  $6 \times 10^{-2}$  and  $8 \times 10^{-2}$  M LiBr, general dissolution also occurs between P1 and P2 while after P2 at 25°C and 50°C metastable pitting was formed which is followed by stable pitting corrosion. Increasing the temperature to 70°C and 80°C, the general dissolution region between P1 and P2 was decreased and after P2 metastable pitting extended to the end of the experiment.
- iv. Further increasing in the concentration of LiBr to  $10^{-1}$  and  $5 \times 10^{-1}$  M, the polarization measurements and surface examination indicates that, as the temperature increases from 25°C to 80°C the general corrosion region between P1 and P2 become very small which decreased by temperature. Here general corrosion represents a small part with respect to pitting corrosion at 80°C, another type of general corrosion is appeared where; a small ratio of Cu<sub>2</sub>O is oxidized to CuO and the film becomes partially protective.

The above results are controlled by different reasons. The first reason is the deficiency in

oxygen soluble in the solution by increasing the temperature which decreases the cathodic reaction. The second is related to the higher increase in diffusion rate and mass transport with increasing the temperature, which tends to increase both the cathodic and anodic reaction. The last reason is related to the dehydration of Cu(OH)<sub>2</sub> to CuO which is more passive and protective enough to prevent general dissolution up to 70°C at  $10^{-1}$  M LiBr. Higher than these temperatures at 80°C and at  $5 \times 10^{-1}$  M of ≥ 50°C, the second type of general corrosion takes place depending on the temperature and the pitting corrosion was disappeared.

### 4.2 Concentrated Solutions of LiBr (From 1 to 9M)

At these higher concentrations of LiBr, the second peak, the passive region and the metastable pitting or pitting corrosion were disappeared, these confirm the general corrosion. As increasing the temperature, the diffusion and mass transport occurs with higher rate, which increases both cathodic and anodic reactions. These become enough to neglect the decrease in the cathodic reaction due to the deficiency in the dissolved oxygen solubility. Accordingly, the dissolution occurs mainly with general form through the complexing formation of CuBr<sub>2</sub><sup>-</sup>.

## COMPETING INTERESTS

Authors have declared that no competing interests exist.

## REFERENCES

1. Igual-Muñoz A, García-Anton J, López S, Guiñón JL, Pérez-Herranz V. Corrosion studies of austenitic and duplex stainless steels in aqueous lithium bromide solution at different temperatures. *Corr. Sci.* 2004; 46:2955.
2. Montanes MT, Sanchez-Tovar R, García-Antón J, Pérez-Herranz V. The influence of reynolds number on the galvanic corrosion of the copper/AISI 304 pair in aqueous LiBr solutions. *Corr. Sci.* 2009;51:2733.
3. Tanno K, Itoh M, Takahashi T, Yashiro H, Kumagai N. The corrosion of carbon steel in lithium bromide solution at moderate temperatures. *Corr. Sci.* 1993;34:1441.

4. Furlong JW. Ozone-friendly chiller boasts many advantages. The Air Pollution Consultant 11/12. Elsevier Science Inc. 1994;1.12–1.14.
5. El Meleigy AE, Shehata MF, Youssef GI, El Hamid ShE, El Warraky AA. Role of Li<sup>+</sup> on the pitting corrosion of copper in LiBr solutions. Ochrona Przed Korozja. 2012; 55:427.
6. Youssef GI, Shehata MF, El Meleigy AE, El Warraky AA, Abd El, Aziz AM. Corrosion and corrosion fatigue behaviour of Al-bronze in LiBr solutions. Ochrona Przed Korozja. 2013;56:34.
7. Khalifa ORM, El Hamid ShE, El Meleigy AE, Shehata MF, El Warraky AA. Corrosion behaviour of Copper in LiBr Solutions. Journal of Scientific Research for Science. 2013;30:34.
8. Munoz-Portero MJ, García-Antón J, Guiñón JL, Pérez-Herranz V. Corrosion of Copper in aqueous Lithium Bromide concentrated solutions by immersion testing. Corrosion. 2006;62:1018.
9. Itzhak D, Greenberg T. Galvanic corrosion of a copper alloy in lithium bromide heavy brine environments. Corrosion. 1995;55: 795.
10. Igual-Munoz A, García-Anton J, Guinon JL, Pérez-Herranz V. Galvanic study of zinc and copper in lithium bromide solutions at different temperatures. Corrosion. 2001;57: 516.
11. Perez-Herranz V, Montanes MT, Garcia-Anton J, Guinon JL. Effect of fluid velocity and exposure time on copper corrosion in a concentrated lithium bromide solution. Corrosion. 2001;57:835.
12. Muñoz-Portero MJ. Copper corrosion in LiBr absorption machines in static and dynamic conditions (Ph.D. Thesis, Universidad Politécnica de Valencia, Spain; 2002.
13. Muñoz-Portero MJ, García-Antón J, Guiñón JL, Pérez-Herranz V. Anodic polarization behavior of copper in concentrated aqueous lithium bromide solutions and comparison with Pourbaix diagrams. Corrosion. 2005;61:464.
14. Montañés MT, Pérez-Herranz V, García-Antón J, Guiñón JL. Evolution with exposure time of copper corrosion in a concentrated lithium bromide solution characterization of corrosion products by energy-dispersive X-ray analysis and X-ray diffraction. Corrosion. 2006;62:64.
15. Blasco–Tamarit E, García-García DM, García-Anton J, Imposed potential measurements to evaluate the pitting corrosion resistance and the galvanic behaviour of a highly alloyed austenitic stainless steel and its weldment in a LiBr solution at temperatures up to 150°C. Corr. Sci. 2011;53:784.
16. Sanchez-Tovar R, Montenes MT, Garcia Anton J. The effect of temperature on the galvanic corrosion of the copper/AISI 304 pair in LiBr solutions under hydrodynamic conditions. Corr. Sci. 2010;52:722.
17. Itzhak D, Greenberg T. Galvanic corrosion of a copper alloy in lithium bromide heavy brine environments. Corrosion. 1999;55(8): 795.
18. Igual-Muñoz A, García-Anton J, Guiñón JL, Pérez-Herranz V. Galvanic studies of copper coupled to alloy 33 and titanium in lithium bromide solutions. Corrosion. 2002;58:995.
19. Igual-Muñoz A, García-Anton J, Guiñón JL, Pérez-Herranz V. Effect of aqueous lithium bromide solutions on the corrosion resistance and galvanic behavior of copper-nickel alloys. Corrosion. 2003;59: 32.
20. Igual-Muñoz A, García-Anton J, Guiñón JL, Pérez-Herranz V. Corrosion behavior and galvanic studies of brass and bronzes in aqueous lithium bromide solutions. Corrosion. 2002;58:560.
21. Munoz-Portero MJ, Garcia-Anton J, Guinon JL, Perez-Herranz V. Analysis of Cu corrosion product in aqueous lithium bromide concentrated solutions. Passivation of Metals and Semiconductors, and Properties of Thin Oxide Layers. Marcus P, Maurice V. (Editors). 2006;131.
22. El Meleigy AE, Abd Elhamid ShE, El Warraky AA. Corrosion behaviour of copper in LiBr solutions-surface examination. Mat.-Wiss.U. Werkstoffech. 2015;46(1):59-68.
23. Valero-Gomez A, Garcia-Anton J, Igual-Munoz A. Corrosion and galvanic behavior of copper and copper-brazed joints in heavy brine lithium bromide solutions. Corrosion. 2006;62:751.
24. Sanchez-Tovar R, Montenes MT. Garcia Anton J. The effect of temperature on the

- galvanic corrosion of the copper/AISI 304 pair in LiBr solutions under hydrodynamic conditions. *Corr. Sci.* 2010;52:722.
25. El Warraky AA, El Shayeb HA, Sherif EM. Pitting corrosion of copper in chloride solutions. *Anti-Corr. Methods and Materials.* 2004;51:52.
  26. Alkire R, Cangellari A. Effect of benzotriazole on dissolution of copper in the presence of fluid flow. *J. Electrochem. Soc.* 1989;136:913.
  27. Deslouis C, Tribollet B, Mengoli G, Musioni MM. Electrochemical behaviour of copper in neutral aerated chloride solution. I. steady-state investigation. *J. Applied Electrochem.* 1988;18:374.
  28. Tang Y, Zuo Yu, Jiani Wang, Xuhui Zhao, Ben Niu, Bing Lin. The metastable pitting potential and its relation to the pitting potential for four materials in chloride solutions. *Corr. Sci.* 2014;80:111–119.
  29. Williams DE, Westcott C, Fleischmann M. Stochastic models of pitting corrosion of stainless steels i.modeling of the initiation and growth of pits at constant potential. *J. Electrochem. Soc.* 1985;132:1796.
  30. Pistorius PC, Burstein GT. Growth of corrosion pits on stainless steel in chloride solution containing dilute sulphate. *Corr. Sci.* 1992;33:1885.
  31. Pistorius PC, Burstein GT. Aspects of the effects of electrolyte composition on the occurrence of metastable pitting on stainless steel. *Corr. Sci.* 1994;36:525.
  32. Frankel GS, Stockert L, Hunkeler F, Boehni H. Metastable pitting of stainless steel. *Corrosion.* 1987;43:429.
  33. Laycock NJ, Newman RC, Localised dissolution kinetics, salt films and pitting potentials. *Corr. Sci.* 1997;39:1771.
  34. Pourbaix M, Klimzack-Mathieiu L, Mertens Ch, Meunier J, Vanleughenaghe Cl, Munck L. de, Laureys J, Neelemans L, Warzee M. Potentiokinetic and corrosimetric investigations of the corrosion behaviour of alloy steels. *Corr. Sci.* 1963;3:239.
  35. Stewart J, Williams DE. The initiation of pitting corrosion on austenitic stainless steel: On the role and importance of sulphide inclusions. *Corr. Sci.* 1992;33: 457.
  36. Coates GE. Effect of some surface treatments on corrosion of stainless steel. *Mater. Perform.* 1990;29:61.
  37. Gupta RK, Sukiman NL, Cavanaugh MK, Hinton BRW, Hutchinson CR, Birbilis N. Metastable pitting characteristics of aluminium alloys measured using current transients during potentiostatic polarization, *Electrochim. Acta.* 2012;66: 245
  38. Williams DE, Stewart J, Balkwill PH. The nucleation, growth and stability of micropits in stainless steel. *Corr. Sci.* 1994;36:1213.
  39. Kim Y, Rudolph G Buchheit. A characterization of the inhibiting effect of Cu on metastable pitting in dilute Al-Cu solid solution alloys, *Electrochimica Acta* 2007, 32, 2437
  40. Becerra JG, Salvarezz RC, Arvia AJ. The influence of slow Cu(OH)<sub>2</sub> phase formation on the electrochemical behaviour of copper in alkaline solutions. *Electrochimica Acta.* 1988;33:613.
  41. Feng Y, Siow KS, Teo WK, Tan KL, Hsieh AK. Corrosion mechanisms and products of copper in aqueous solutions at various pH values. *Corrosion.* 1997;53:389.
  42. Fernandez-Domene RM, Blasco-Tamarit E, García-García DM, García-Anton J. Thermogalvanic effects on the corrosion of copper in heavy brine LiBr solutions. *Corr. Sci.* 2012;63:304.
  43. Frankel GS, Sridhar N. Understanding localized corrosion. *Mater. Today.* 2008; 11:38–44.
  44. Aben T, Tromans D. Anodic polarization behavior of copper in aqueous bromide and bromide/benzotriazole solution. *J. Electrochem. Soc.* 1995;142:398.
  45. Igual Muñoz A, García Antón J, Guiñón JL, Pérez Herranz V. Effects of solution temperature on localized corrosion of high nickel content stainless steels and nickel in chromated LiBr solution. *Corr. Sci.* 2006;48:3349.
  46. Dong ZH, Shi W, Zhang GA, Guo XP. The role of inhibitors on the repassivation of pitting corrosion of carbon steel in synthetic carbonated concrete pore solution. *Electrochim. Acta.* 2011;56:5890.
  47. Burstein GT, Pistorius PC, Mattin SP. The nucleation and growth of corrosion pits on stainless steel, *Corr. Sci.* 1993;35:57.
  48. Pistorius PC, Burstein GT. Metastable pitting corrosion of stainless-steel and the transition to stability. *Philos. Trans. Roy. Soc.* 1992;A(341):531.

49. Pistorius PC, Burstein GT. Detailed investigation of current transients from metastable pitting events on stainless steel- the transition to stability, Mater.Sci. Forum. 1992;111:429.
50. Starosvetsky D, Khaselev O, Auinat M, Ein-Eli Y. Initiation of copper dissolution in sodium chloride electrolytes. Electrochimica Acta. 2006; 51:5660.

---

© 2015 Meleigy et al.; This is an Open Access article distributed under the terms of the Creative Commons Attribution License (<http://creativecommons.org/licenses/by/4.0>), which permits unrestricted use, distribution, and reproduction in any medium, provided the original work is properly cited.

*Peer-review history:*  
*The peer review history for this paper can be accessed here:*  
<http://sciencedomain.org/review-history/11222>